JOURNAL OF APPLIED POLYMER SCIENCE VOL. 20, 2165–2182 (1976)

Mechanical Dispersion of Crosslinked Polymers Reinforced with Randomly Distributed Short Fiber

MINEKAZU KODAMA, *Manufacturing Development Laboratory, Mitsubishi Electric Corporation, Minamishimizu, Amagasaki, Hyogo, Japan*

Synopsis

The dynamic viscoelastic properties of composites reinforced with randomly distributed short glass and carbon fibers were studied in relation to the dependence on the fiber length, the mixing ratio of glass fibers of different length, and the kind of polymer matrix. Although the composite reinforced with glass fiber of 0.05 mm in length shows only one dispersion (α) corresponding to the primary transition of polymer matrix, those reinforced with 3- and 10-mm glass fibers, and those reinforced with the mixture of 10- and 0.05-mm glass fibers are characterized by two additional dispersions (α' and α'') which appear on the lower frequency side or higher temperature side of the α-dispersion. The composite reinforced with 3-mm carbon fiber does not show the additional dispersions. The α'- and α''-dispersions appear irrespective of the kind of matrix polymer.

INTRODUCTION

The nature and the extent of the interaction between polymer matrix and reinforcing material is well known to have an important bearing on the mechanical properties of polymeric composites. For instance, the mechanical loss tangent or loss modulus and the mechanical energy dissipation associated therewith have been shown to be delicately affected by the differences in the nature and extent of the interaction between polymer matrix and reinforcing material for the cases of particulate composites.[1] However, the study concerning the mechanical energy dissipation is relatively rare for fiber composites.[2]

In this work, the dynamic viscoelastic properties of composite reinforced with randomly distributed short fiber were studied. The primary object of this work is to inquire into the mechanical dispersion behavior of crosslinked polymers reinforced with short glass and carbon fibers of random-planar distribution in relation to the dependence on fiber length, the mixing ratio of fibers of different length, and the kind of polymer matrix. Because the presence of reinforcing material in relatively large concentration can considerably obscure the effect of matrix-reinforcing material interface, composites reinforced with relatively small concentrations of fibers are used in this study.

EXPERIMENTAL

Reinforcing fibers used in this work were E-glass fibers 0.05, 3, and 10 mm long (Nittobo Co.) and resinous pitch carbon fiber 3 mm long (Kureha Co.).

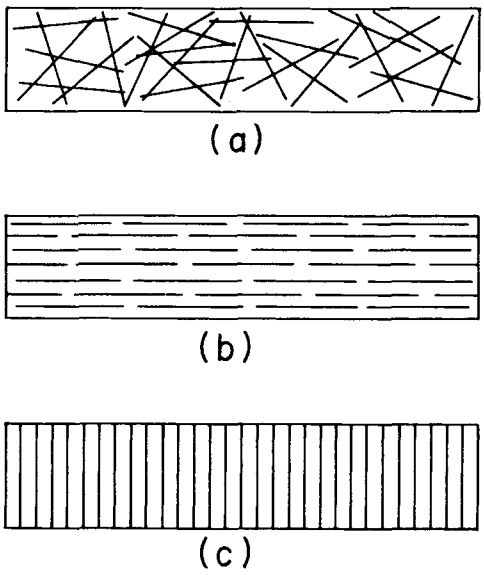

Fig. 1. Schematic representation of composites reinforced with randomly distributed fibers (a), with uniaxially aligned fibers in the direction of sample length (b), and with perpendicularly aligned fibers to the direction of sample length (c).

Diameters of glass and carbon fibers were 9 and 10 μm, respectively. The fibers had no surface treatment.

Styrene-modified epoxy resin, bisphenol-type epoxy resin, Epikote 828 (Shell Chemical Co.) cured with nadic methyl anhydride, and methyl methacrylate resin crosslinked with ethylene glycol dimethacrylate were used as polymer matrix. Styrene-modified epoxy resin is widely used as the matrix of FRP because of good processability and performance. Styrene-modified epoxy resin was prepared as follows: Unsaturated polyester oligomer having an acid value of 110 was synthesized from a mixture of maleic anhydride, phthalic anhydride, isophthalic anhydride, and ethylene glycol of 0.5, 0.2, 0.3 and 1.0 mole ratio, respectively, by esterfication reaction at 160°C. Then, 125 parts by weight of Epikote 828 was mixed with 150 parts by weight of the unsaturated polyester oligomer, and the reaction was continued at 150°C until a resinous product of acid value 35 was obtained. Finally, the thus prepared reaction product was dissolved by styrene monomer at a concentration of 45% by weight.

The composite reinforced with 0.05-mm glass fiber was prepared by directly mixing the fiber, which was dried at 100°C before use, with resin matrix. The composites reinforced with 3- and 10-mm fibers were prepared by impregnating the random-planar fiber mat with resin matrix. The random-planar fiber mat was obtained by uniformly and randomly dispersing the fiber in a large volume of water in which 1% poly(vinyl alcohol) was dissolved as the binder of fiber, then scooping up the dispersed fiber on wire netting, and finally drying at 100°C the scooped fibers between glass plates at the slightly compressed state.

The composites reinforced with a mixture of 0.05- and 10-mm glass fibers were prepared by uniformly sprinkling 0.05-mm fiber through wire netting of

TABLE I
Composition and Cure Condition of Samples

Code	Matrix (mixing ratio in weight)	Reinforcement		Cure conditions
		Kind (fiber length, mm)	Content, vol-%	
S	styrene-modified epoxy resin	—	0	(100° C, 2 hr) + (135° C, 4 hr)
S-MG-8		milled glass fiber (0.05)	8	
S-3G-5		E-glass fiber (3)	5	
S-3C-5		resinous pitch carbon fiber (3)	5	
S-10G-4		E-glass fiber (10)	4	
S-10G-7P[a]		E-glass fiber (10)	7	
S-5G-7V[b]		E-glass fiber (5)	7	
B	Epikote 828/nadic methyl anhydride (10/9)	—	0	(100° C, 2 hr) + (150° C, 7 hr)
B-10G-4		E-glass fiber (10)	4	
B-3C-4		resinous pitch carbon fiber (3)	4	
B-10G/P-2/0		mixture of E-glass fiber (10) and milled E-glass fiber (0.05)	2.4 (10/M = 2.4/0)[c]	
B-10G/P-2/5			7.4 (10/M = 2.4/5)	
B-10G/P-2/10			12.5 (10/M = 2.4/10.1)	
B-10G/P-1/6			6.9 (10/M = 1.2/5.7)	
B-10G/P-3/6			8.3 (10/M = 2.6/5.7)	
B-10G/P-5/6			10.7 (10/M = 5.0/5.7)	
M-10G-5	methyl methacrylate/ ethylene glycol dimethacrylate (95/5)	E-glass fiber (10)	5	(100° C, 1 hr) + (140° C, 4 hr)

[a] Fiber is uniaxially aligned in the direction of sample length as shown schematically in Figure 1b.
[b] Fiber is perpendicularly aligned to the direction of sample length as shown schematically in Figure 1c.
[c] 10/M means mixing ratio of glass fiber 10 mm long to milled glass fiber.

80 mesh on the random-planar mat and then by impregnating this two-phase reinforcement with resin matrix.

For the sake of comparison with randomly distributed composites, uniaxially oriented fiber composites were also prepared by aligning glass fiber uniaxially and then pouring resin matrix on to the fiber array, as shown schematically in Figures 1b and 1c. Randomly distributed composite was also shown schematically in Figure 1a.

The composites prepared here had a form of sheet of thickness 0.3–0.6 mm. The composition and cure condition of composites are shown in Table I together with the sample code.

The dynamic viscoelastic properties were measured using a viscoelastic spectrometer VES (Iwamoto Seisakusho Co.). The complex dynamic tensile modulus was obtained above room temperature over a frequency range of 1 to 40 Hz. The measurements were made by superposing a dynamic tensile strain less than 0.7% on a static tensile strain of 1%.

RESULTS AND DISCUSSION

Frequency Dispersion of Loss Modulus

The frequency dependence of the loss modulus at various temperatures is shown for selected samples in Figures 2 to 4. It is noted that the primary dispersion (α-dispersion), associated with the glass–rubber transition of the polymer matrix, can be seen at around 100° and 120°C for S-3G-5 and B composites, respectively. The results of the other samples were omitted for saving space. Although the dispersion temperature is hardly affected by the differences of fiber length and fiber content, the shape of the curve is delicately affected by these factors.

Time–Temperature Superposition

Although the correction for the temperature and density ($T\rho/T_0\rho_0$) was neglected, time-temperature superposition seemed possible for the loss modulus

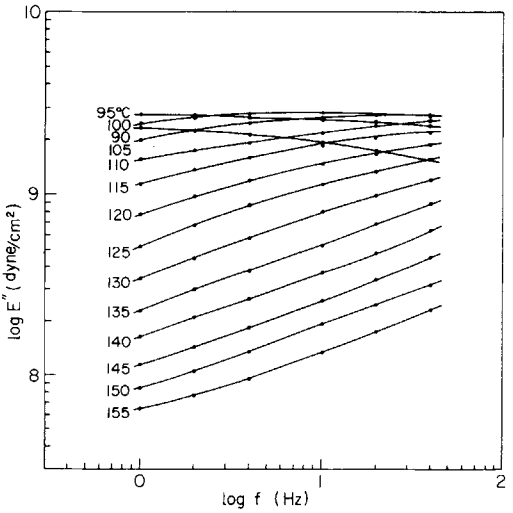

Fig. 2. Frequency dispersion of loss modulus at various temperatures for S-3G-5.

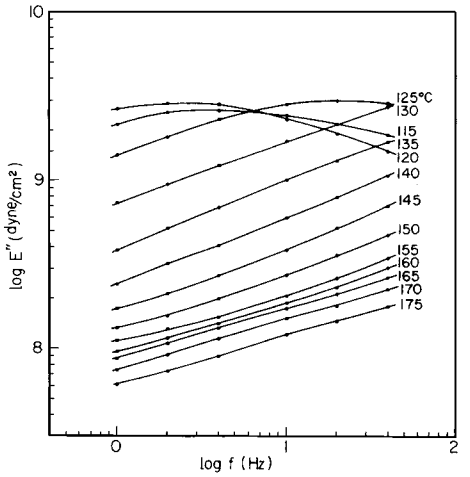

Fig. 3. Frequency dispersion of loss modulus at various temperatures for B-10G-4.

data over the α-dispersion temperature except for S-10G-4 and M-10G-5. For the cases of S-10G-4 and M-10G-5, time–temperature superposition could not be possible.

Figures 5 and 6 show the temperature dependence of the shift factor for composing master loss modulus curve as a check of the linear relationship of the WLF equation, assuming temporarily the validity of the time–temperature superposition. The linear relationship of the WLF equation is given by eq. (1):

$$(T - T_0)/\log a_T = -(C_2/C_1) - (T - T_0)/C_1. \quad (1)$$

In eq. (1), T_0 is the reference temperature at which the superposition was carried out, and C_1 and C_2 are constants. As seen in Figures 5 and 6, the agreement of the temperature dependence of the shift factor $\log a_{T_\alpha}$ with that pre-

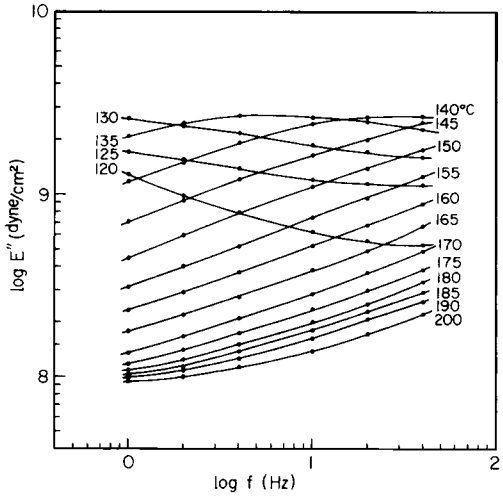

Fig. 4. Frequency dispersion of loss modulus at various temperatures for B-10G/P-5/6.

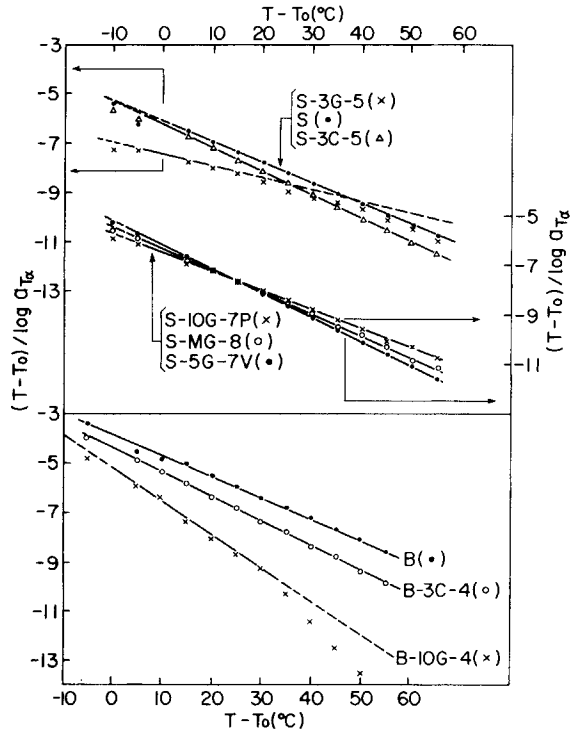

Fig. 5. Temperature dependence of shift factor log a_{T_α} for composing master loss modulus curves from frequency dispersion of loss modulus.

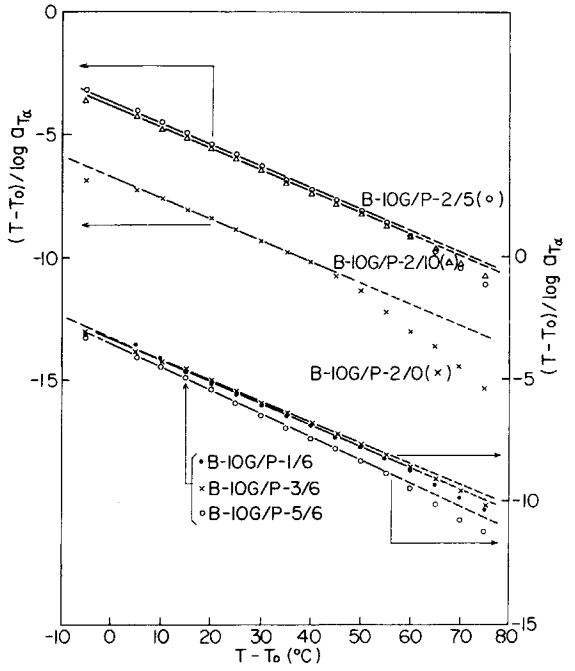

Fig. 6. Temperature dependence of shift factor log a_{T_α} for composing master loss modulus curves from frequency dispersion of loss modulus.

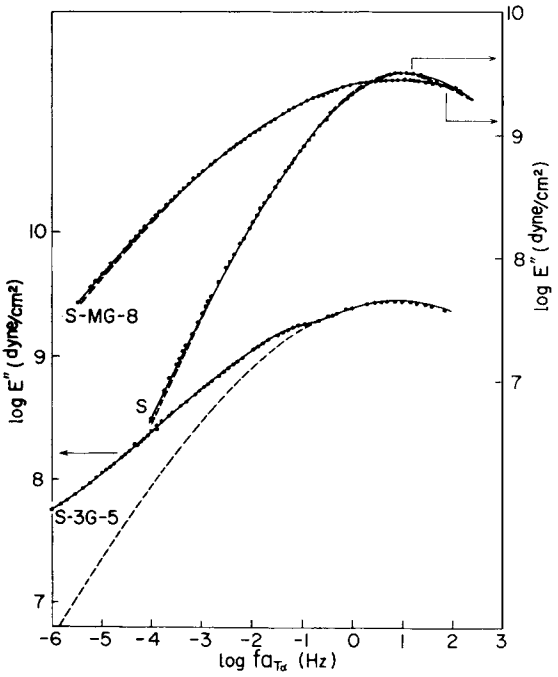

Fig. 7. Master loss modulus curves. Reference temperature of each sample is 100°C. The curve of S-3G-5 was recomposed in accordance with shift factor log a_{T_α} given by the linear relationship and its extrapolation in Fig. 5. Broken curves are the Gaussian function to hit the primary dispersion for each sample as closely as possible.

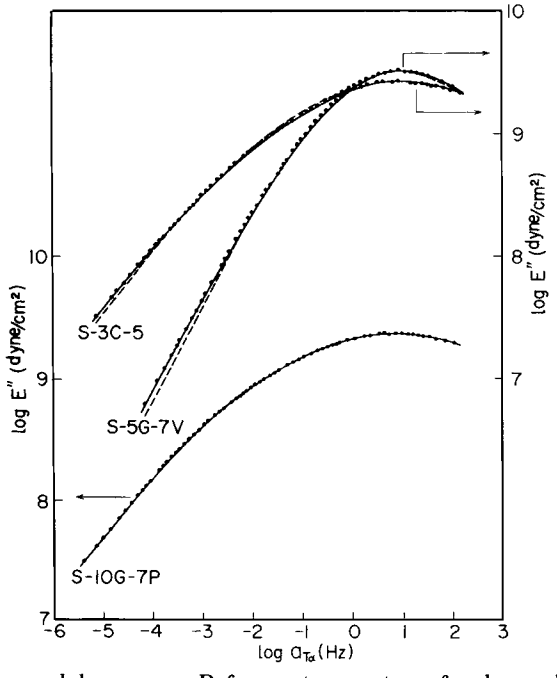

Fig. 8. Master loss modulus curves. Reference temperature of each sample is 100°C. Broken curves are the Gaussian function to hit the primary dispersion for each sample as closely as possible.

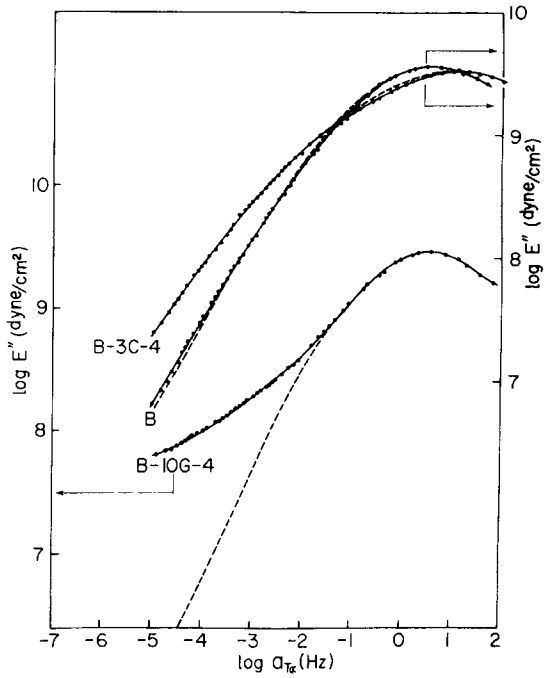

Fig. 9. Master loss modulus curves. Reference temperature of each sample is 125°C. Curve of B-10G-4 was recomposed in accordance with shift factor log a_{T_α} given by the linear relationship and its extrapolation in Fig. 5. Broken curves are the Gaussian function to hit the primary dispersion for each sample as closely as possible.

dicted from the WLF equation is quite good for S, S-MG-8, S-3C-5, S-10G-7P, S-5G-7V, B, and B-3C-4. The linear relationship does not hold for other samples and shows a gradual deviation from the linear relationship with increase in temperature. Such a deviation is observed irrespective of reference temperature for these samples.

The gradual deviation from the linear relationship suggests the existence of other kinds of relaxation processes.[3] If this is the case, the procedure of time–temperature superposition carried out temporarily should be invalid. Therefore, the "valid" master loss modulus curves[3] were constructed by superposing again the original results, such as in Figures 2 to 4, according to the temperature dependence of the shift factor given by the linear relationship and its extrapolations indicated by the broken lines in Figures 5 and 6. Thus obtained master loss modulus curves are shown in Figures 7 to 11, together with the cases of S, S-MG-8, S-3C-5, S-10G-7P, S-5G-7V, B, and B-3C-4. For S-3G-5, another broad dispersion is seen as a shoulder on the low-frequency side of the α-dispersion. For B composites, except for B-3C-4, the master loss modulus curves become flatter gradually as the reduced frequency is lowered.

Temperature Dispersion of Loss Modulus

As mentioned above, the procedure of time–temperature superposition cannot be applied for S-10G-4 and M-10G-5. Therefore, the loss modulus

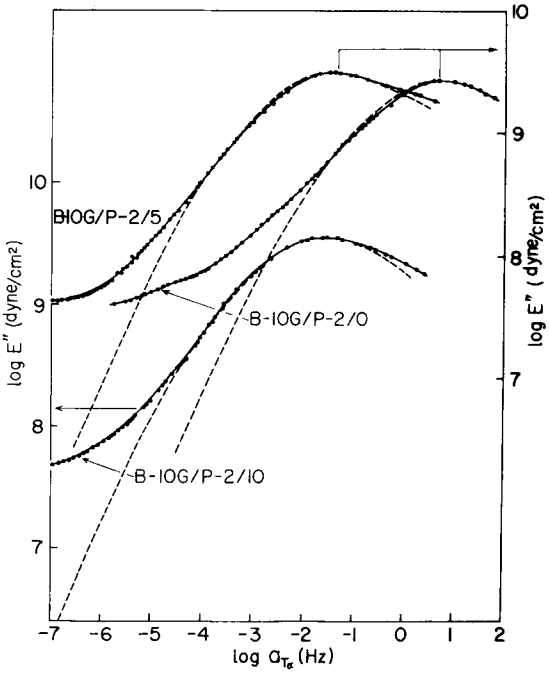

Fig. 10. Master loss modulus curves. Reference temperature of each sample is 125°C. Curves were recomposed in accordance with shift factor log a_{T_α} given by the linear relationship and its extrapolation in Fig. 6. Broken curves are the Gaussian function to hit the primary dispersion as closely as possible.

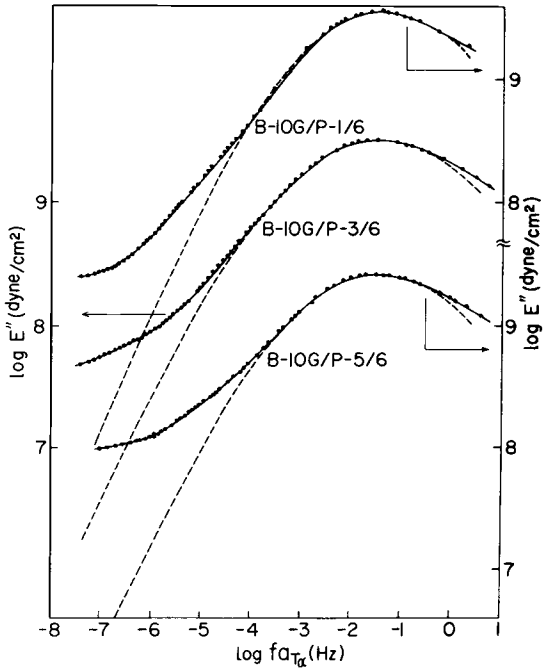

Fig. 11. Master loss modulus curves. Reference temperature of each sample is 125°C. Curves were recomposed in accordance with shift factor log a_{T_α} given by the linear relationship and its extrapolation in Fig. 6. Broken curves are the Gaussian function to hit the primary dispersion as closely as possible.

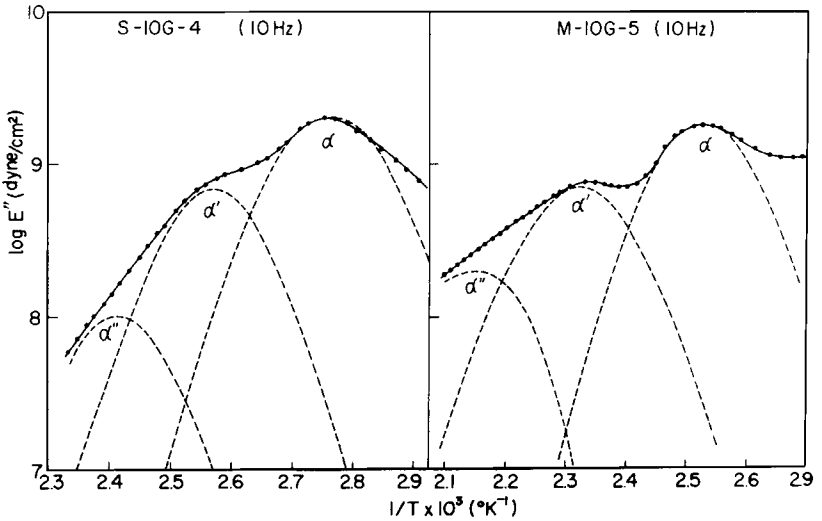

Fig. 12. Temperature dependence of loss modulus for S-10G-4 and M-10G-5. Broken curves are the Gaussian function corresponding to each dispersion.

was plotted in Figure 12 as a function of temperature at fixed frequency. A hump is seen at the higher-temperature side of the α-dispersion for both composites.

Separation of Additional Dispersions from Master Loss Modulus Curves

In the above section, the existence of relaxation processes other than the α-process was suggested for S-3G-5, B-10G-4, B-10G/P-2/0, B-10G/P-2/5, B-10G/P-2/10, B-10G/P-1/6, B-10G/P-3/6, and B/10G/P-5/6. In this section, the separation of additional dispersions for these composites was tried according to the procedure of Tajiri et al.[3] This procedure seemed to have succeeded in the separation of various relaxation mechanisms for many kinds of samples.[3–5]

The procedure is based on the following three assumptions: (1) additivity for assessing the contribution of each relaxation mechanism of the viscoelastic functions, (2) validity of the time–temperature superposition hypothesis within each mechanism independently of other mechanism, and (3) a Gaussian-type symmetric function with respect to double-logarithmic plots of frequency and loss modulus for each mechanism, i.e.,

$$\log E'' = A \exp\{-C(\log f - \log f_0)^2\} \tag{2}$$

where A, C, and f_0 are constants to characterize the Gaussian-type function, i.e., the logarithmic value of the maximum loss modulus, the parameter representing the sharpness of the dispersion and the reduced frequency at which the loss modulus takes the maximum value, respectively.

The broken lines in Figures 7 to 11 are the Gaussian function to fit the α-dispersion for each samples as closely as possible. The constants characterizing the Gaussian functional form are listed in Table II.

TABLE II
Constants Characterizing the Gaussian Functional Form for the Frequency Dispersion of Loss Modulus and Temperature Dependence of Shift Factor

Code	Dispersion	A	log f_0	C	T_0, °C	$C_1°$	$C_2°$	ΔH^*, kcal/mole
S	α	9.50	0.90	0.0165	100	11.8	61.4	—
S-MG-8	α	9.44	0.90	0.0056	100	11.1	59.9	—
	α	9.44	0.90	0.0071		21.7	151.9	—
S-3G-5	α'	9.52	−2.50	0.0195	100	—	—	101.2
	α''	7.98	−5.50	0.0198		—	—	101.4
S-3C-5	α	9.43	1.00	0.0065	100	10.4	54.0	—
S-10G-7P	α	9.37	0.90	0.0059	100	12.8	72.3	—
S-5G-7V	α	9.51	0.90	0.0144	100	10.1	52.0	—
B	α	9.56	0.70	0.0120	125	11.4	43.3	—
	α	9.46	0.60	0.0167		7.3	37.6	—
B-10G-4	α'	8.16	−3.90	0.0137	125	—	—	94.5
	α''	7.78	−6.10	0.0215		—	—	98.9
B-3C-4	α	9.52	1.00	0.0075	125	10.0	43.3	—
	α	9.43	0.70	0.0145		11.6	77.7	—
B-10G/P-2/0	α'	7.98	−3.10	0.0164	125	—	—	85.0
	α''	7.63	−6.30	0.0230		—	—	85.2
	α	9.50	−1.50	0.0156		11.2	42.1	—
B-10G/P-2/5	α'	7.76	−5.55	0.0165	125	—	—	101.0
	α''	7.53	−8.50	0.0225		—	—	102.0
	α	9.56	−1.60	0.0145		11.3	44.1	—
B-10G/P-2/10	α'	7.77	−6.00	0.0355	125	—	—	97.0
	α''	7.68	−8.65	0.0225		—	—	98.0
	α	9.57	−1.40	0.0143		10.8	34.0	—
B-10G/P-1/6	α'	7.80	−5.00	0.0155	125	—	—	103.0
	α''	7.38	−8.10	0.0220		—	—	108.0
	α	9.51	−1.50	0.0125		11.1	35.5	—
B-10G/P-3/6	α'	7.79	−5.30	0.0155	125	—	—	116.0
	α''	7.70	−8.15	0.0210		—	—	116.8
	α	9.42	−1.50	0.0136		10.2	34.7	—
B-10G/P-5/6	α'	8.18	−5.10	0.0155	125	—	—	105.8
	α''	7.95	−8.20	0.0202		—	—	107.9

The master loss modulus curves of polymer matrix (S and B) and composites reinforced with milled-glass fiber (S-MG-8), with carbon fiber (S-3C-5 and B-3C-4), and with uniaxially aligned glass fiber (S-10G-7P and S-5G-7V) fit very well the Gaussian functions over the whole frequency range, as shown in Figures 7 to 11. The constants characterizing these Gaussian functions are also listed in Table II.

As in the cases of S-3G-5, B-10G-4, B-10G/P-2/0, B-10G/P-2/5, B-10G/P-2/10, B-10G/P-1/6, B-10G/P-3/6, and B-10G/P-5/6, the deviation of the master loss modulus curves from the Gaussian function at the low reduced-frequency side should be considered as a contribution from another relaxation mechanism. The temperature dependence of the shift factor log $a_{T_{\alpha'}}$ for recomposing the master loss modulus curve of this additional relaxation mechanism from the residue of the Gaussian function, on the low-frequency side in Figures 7 to 11, is plotted in Figure 13 against the reciprocal temperature by taking the previous shift factor log a_{T_α} into account for selected samples. As seen in Figure 13, the plots deviate from a linear relationship with increase in

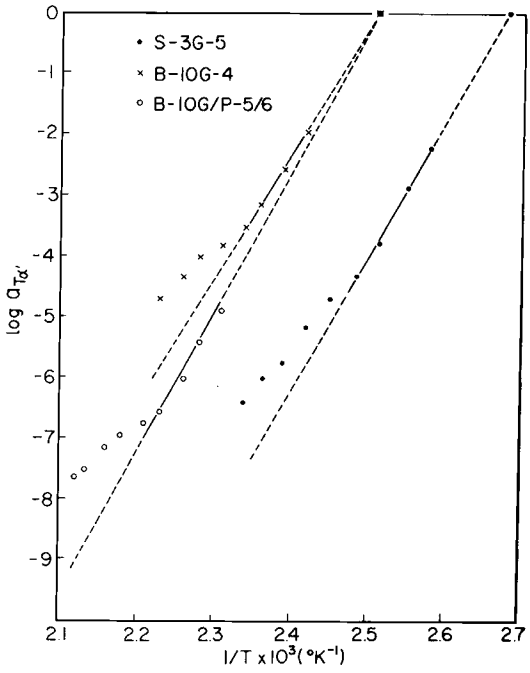

Fig. 13. Temperature dependence of shift factor log $a_{T_{\alpha'}}$ for recomposing the master loss modulus curve of additional relaxation mechanism.

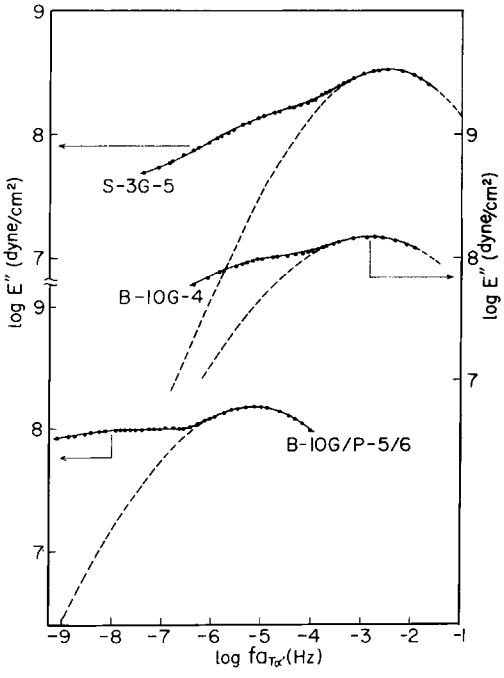

Fig. 14. Master loss modulus curves of additional relaxation mechanism superposed in accordance with shift factor log $a_{T_{\alpha'}}$ given by the linear relationship and its extrapolation in Fig. 13. Broken curves are the Gaussian function to hit the dispersion (α') as closely as possible.

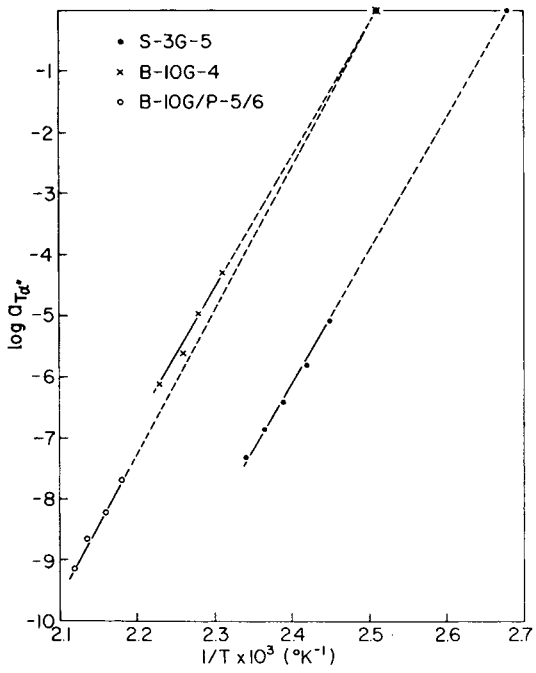

Fig. 15. Temperature dependence of shift factor log $a_{T_{\alpha''}}$ for recomposing master loss modulus curve of additional relaxation mechanism from the residue of the Gaussian function on the low-frequency side in Fig. 14.

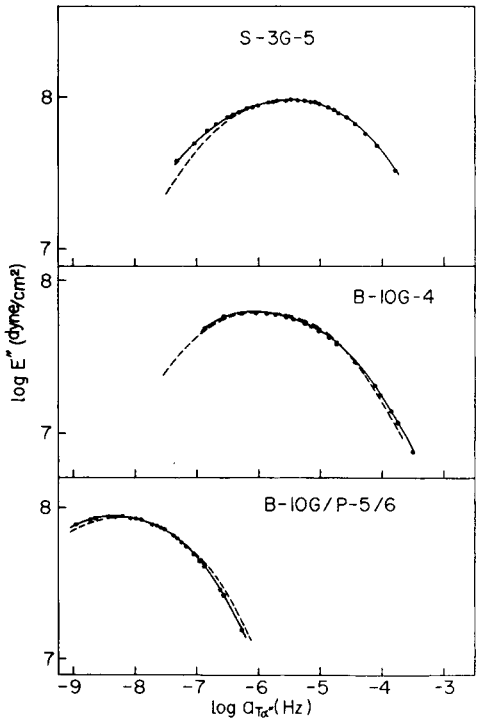

Fig. 16. Master loss modulus curves superposed in accordance with shift factor log $a_{T_{\alpha''}}$. Broken curves are the Gaussian function to hit the dispersion (α'') as closely as possible.

temperature. Figure 14 shows the master loss modulus curves of the additional relaxation mechanism recomposed in accordance with the shift factor log $a_{T_{\alpha'}}$ giving by the linear relationship and its extrapolation to lower reciprocal temperature. As seen in Figure 14, the master loss modulus curves are asymmetric with respect to the reduced frequency. The broken lines in Figure 14 are the Gaussian function of the additional relaxation mechanism (α'-dispersion) drawn by using the same procedure as that for the α-relaxation mechanism. The constants characterizing the Gaussian functional form are also listed in Table II.

Again, by considering that the deviation of the master loss modulus curve from the Gaussian function as seen in Figure 14 is the contribution from an additional relaxation mechanism to the loss modulus, the separation of an additional relaxation mechanism was made. The temperature dependence of the shift factor log $a_{T_{\alpha''}}$ for recomposing the master loss modulus curve of the additional relaxation mechanism is plotted in Figure 15. The plots can be represented by a linear relationship. That is, the temperature dependence is given by an Arrhenius-type equation. The master loss modulus curves thus obtained for the additional relaxation mechanism (α''-dispersion) can be represented by a symmetric function as shown in Figure 16. The constants characterizing the Gaussian functional form are listed in Table II.

The separation of the additional relaxation mechanisms was also made in accordance with the above procedure for B-10G/P-2/0, B-10G/P-2/5, B-10G/P-2/10, B-10G/P-1/6, and B-10G/P-3/6. The α'- and α''-dispersions can also be separated in these composites as listed the constants characterizing these dispersions in Table II.

The constants characterizing the temperature dependence of shift factors, T_0, C_1, C_2, and ΔH_a, are also listed in Table II. C_1 and C_2 were obtained from the linear relationship and its extrapolation given by the broken lines in Figures 5 and 6. The activation energy ΔH_a of the α'-dispersion was obtained from the slope of linear lationship and its extrapolation to lower reciprocal temperature, as shown in Figure 13, and that of the α''-dispersion was obtained from the slope of the linear relationship in Figure 15.

Separation of Additional Dispersions from Temperature Dispersion of Loss Modulus

The additional dispersions of S-10G-4 and M-10G-5 were separated from the log E''-versus-1/T curves as shown in Figure 12 by broken lines. The procedure of separation[6] is similar to that of the above section. In this case, a Gaussian-type symmetric function given by eq. (3) was used by assuming the Arrhenius-type equation for the temperature dependence of the shift factor:

$$\log E'' = A \exp\left\{-C\left(\frac{1}{T} - \frac{1}{T_r}\right)^2\right\} \tag{3}$$

where $1/T_r$ is the reciprocal temperature at which the loss modulus takes the maximum value. As seen in Figure 12, a hump observed at the higher-temperature side of the α-dispersion was decomposed into two dispersions (α' and α'') for both composites. The constants characterizing the Gaussian

TABLE III
Constants Characterizing the Gaussian Functional Form for the Temperature Dispersion of Loss Modulus

Code	Dispersion	A	$1/T_r \times 10^3$	$C \times 10^{-8}$
	α	9.30	2.765	0.0392
S-10G-4	α'	8.83	2.575	0.0476
	α''	8.01	2.420	0.0555
	α	9.27	2.530	0.0460
M-10G-5	α'	8.85	2.325	0.0395
	α''	8.29	2.145	0.0361
S-3C-5	α	9.48	2.795	0.0289
	α	9.40	2.760	0.0398
S-3G-5	α'	8.88	2.610	0.0690
	α''	8.14	2.485	0.0775
Additionally	α	9.45	2.735	0.0477
cured S-3G-5	α[a]	8.56	2.475	0.0620
	α	9.38	2.770	0.0320
S-3G-5F_1	α'	8.30	2.585	0.0547
	α''	7.58	2.465	0.0904
S-3G-5F_2	α	9.38	2.770	0.0320
	α[b]	7.76	2.545	0.1000

[a] Corresponds to the α''-dispersion of S-3G-5.
[b] Corresponds to the α'-dispersion of S-3G-5.

functional form of each dispersion are listed in Table III. The fitting of eq. (3) to the log E''-versus-$1/T$ curve of S-3C-5 and S-3G-5 was also tried, as shown in Figure 17. The curve of S-3C-5 is well represented by one Gaussian function over the whole temperature range, and that of S-3G-5 is decomposed into three Gaussian functions.

Effects of Additional Curing and Fatigue on the Dispersions

In Figure 17, the result of separation of the additional dispersion from the log E''-versus-$1/T$ curve was shown for the additionally cured S-3G-5. The additional curing was carried out at 130°C for 5 hr. By additional curing, though the α'-dispersion disappears, the dispersion corresponding to the α''-dispersion remains. The storage modulus at the rubbery region is increased from 3.0×10^9 dynes/cm^2 to 4.0×10^9 dynes/cm^2 accompanied with the additional curing.

In Figure 18, the result of separation of the additional dispersions was shown for the fatigued S-3G-5. The fatigue was given by subjecting to cyclic tensile loading of the mean stress of 0.6 kg/mm^2 (mean strain 0.2%) at the rate of cycling of 6000 rpm. S-3G-5F_1 and S-3G-5F_2 represent the specimens subjected to the number of cycles of 5×10^4 and 1×10^5, respectively. The α'- and α''-dispersions of S-3G-5F_1 become smaller than those of S-3G-5. For S-3G-5F_2, the dispersion corresponding to the α'-dispersion is observed only, and this dispersion is smaller than the α'-dispersion of S-3G-5F_1. The storage moduli at the rubbery region of S-3G-5F_1 and S-3G-5F_2 are 2.5×10^9 dynes/cm^2 and 2.0×10^9 dynes/cm^2, respectively. That is, the storage modulus at the rubbery region is decreased with progression in fatigue. The storage modulus at the rubbery region of the S sample is little affected by the fa-

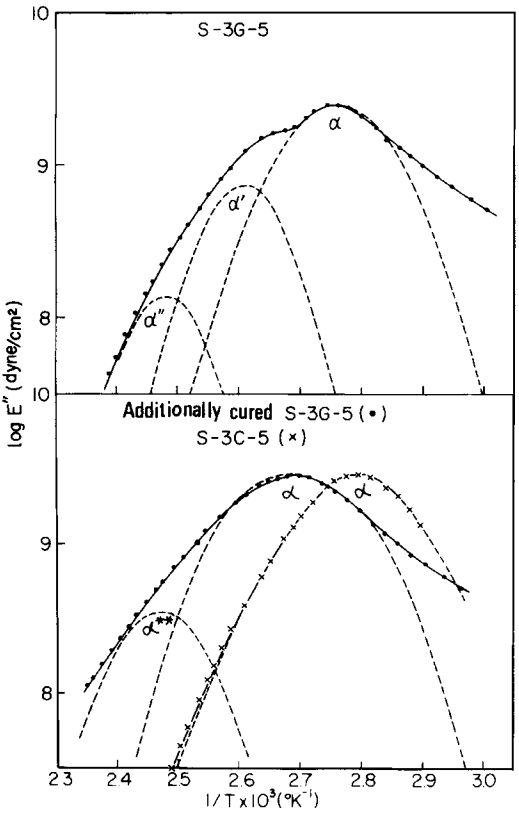

Fig. 17. Temperature dependence of loss modulus for S-3G-5, additionally cured S-3G-5, and S-3C-5. Broken curves are the Gaussian function to hit each dispersion as closely as possible; α^{**} shows the dispersion corresponding to the α''-dispersion of S-3G-5.

tigue. These facts suggest that the decrease in the storage modulus at rubbery region and, further, the diminution of the additional dispersions accompanied by fatigue are mainly caused by the change in the fiber–matrix interaction.

Deduction of Mechanism for α'- and α''-Dispersions

As shown above, the α'- and α''-dispersions appear for the composites reinforced with randomly distributed glass fiber longer than 3 mm and those reinforced with mixtures of randomly distributed glass fiber 10 mm and 0.05 mm long. The composites reinforced with randomly distributed carbon fiber do not show the α'- and α''-dispersions. This is probably because of the weaker interaction[7] of carbon fiber with the resin matrix as compared with the case of glass fiber. The weakness of the interaction of carbon fiber with the resin matrix is also apparent from the fact that the storage modulus at rubbery region of S-3G-5 is three times larger than that of S-3C-5.

From these facts it is considered that the intersection among the fibers and the relatively strong interaction between the resin matrix and the fiber is necessary for the occurrence of the α'- and α''-dispersions.

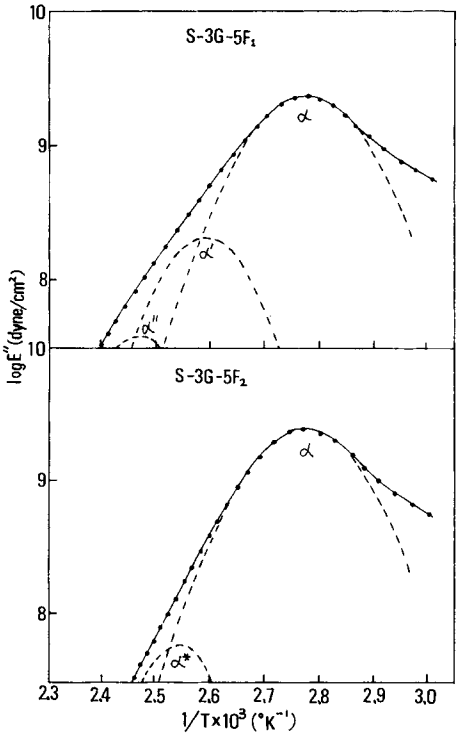

Fig. 18. Temperature dependence of loss modulus for fatigued S-3G-5. Broken curves are the Gaussian function to hit each dispersion as closely as possible; α^* shows the dispersion corresponding to the α'-dispersion of S-3G-5.

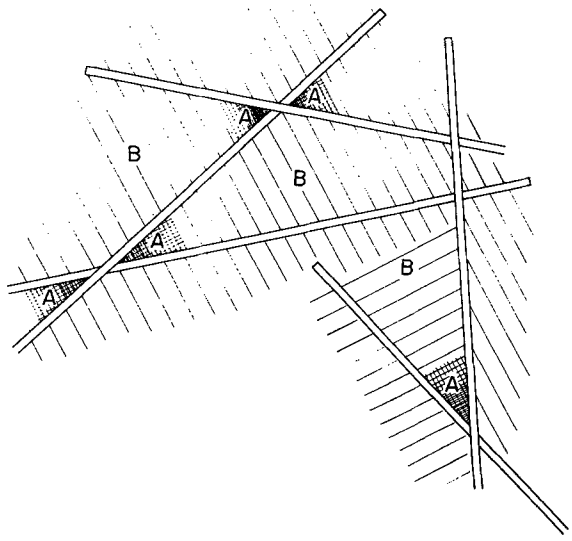

Fig. 19. Schematic representation of the intersections of glass fibers in composite.

Figure 19 shows schematically the intersection of glass fibers in the composite. The matrix resin penetrated in such a region as A, which is part of the space partitioned by the intersected fibers at an acute angle, is considered to be strongly constrained as to mobility compared with the resin matrix present in a space as extensive as B. Therefore, the solid structure of decreased mobility or higher transition temperature is considered to be possibly formed in region A by curing. The strucutre of region A seemed to be responsible for the α'-dispersion. For the additionally cured sample, the dispersion corresponding to the α'-dispersion disappears. It would seem that the polymer has cured fully and therefore cannot relax locally at the temperature corresponding to the α'-dispersion temperature of the original sample. When the fiber–matrix interaction is weakened by fatigue, the structure of region A is considered to become less constrained as to mobility, and consequently the strength of the dispersion will be diminished.

If the temperature is further increased above the transition temperature of the structure of region A or the frequency is reduced below the dispersion region of the structure of region A, friction or slippage between the glass fiber and the resin matrix of region A is considered to arise. This friction or slippage can be an energy dissipation mechanism and is possibly observed as a dispersion because the energy dissipation based on the primary transition of polymer matrix is considered to be relatively small in the temperature or frequency region. Such a mechanism seems to be mainly responsible for the α''-dispersion. For the additionally cured S-3G-5, the dispersion corresponding to the α''-dispersion seems to arise from the combined effects of the transition in the fully cured structure with the friction or slippage between glass fiber and resin matrix of region A. For the fatigued sample, it is considered that the fiber–matrix interaction is so weakened that friction or slippage between fiber and matrix hardly contribute to the energy dissipation mechanism. For S-3C-5 and B-3C-4, a structure such as region A is not formed on account of weaker interaction between carbon fiber and matrix as mentioned above, and therefore the α''-mechanism cannot appear. For S-10G-7P and S-5G-7V, the intersection among the glass fibers is not found. Therefore, a structure such as region A cannot be formed.

References

1 T. B. Lewis and L. E. Nielsen, *J. Appl. Polym. Sci.*, **14,** 1449 (1970); L. E. Nielsen and B. Lee, *J. Composite Mater.*, **6,** 136 (1972).

2 A. B. Schultz, *J. Composite Mater.*, **2,** 368 (1968); M. Schrager and J. Carey, *Polym. Eng. Sci.*, **10,** 369 (1970).

3 K. Tajiri, Y. Fujii, M. Aida, and H. Kawai, *J. Macromol. Sci.-Phys.*, **B4**(1), 1 (1970).

4 T. Soen, T. Ono, K. Yamashita, and H. Kawai, *Kolloid-Z. Z. Polym.*, **250,** 459 (1972).

5 T. Soen, M. Shimomura, T. Uchida, and H. Kawai, *Colloid Polym. Sci.*, **252,** 933 (1974).

6 H. Kawai, in *Reorojii Nyumon,* S. Oka, Ed., Kogyo Chosa Kai, Tokyo, 1970, p. 137.

7 J. P. Favre and J. Perrin, *J. Mater, Sci.*, 1113 (1972).

Received August 8, 1975
Revised October 15, 1975